

Unitarity and Dark Matter in the Private Higgs Model

C. B. Jackson*

Physics Department, Brookhaven National Laboratory, Upton, NY 11973-5000, USA

(Dated: June 21, 2024)

Abstract

The extremely large hierarchy observed in the fermion mass spectrum remains as one of the most puzzling and unresolved issues in particle physics. In a recent proposal, however, it was demonstrated that by introducing one Higgs doublet (or *Private Higgs*) per fermion this hierarchy could be made natural by making the Yukawa couplings between each fermion and its respective Higgs boson of order unity. Among the interesting predictions of the Private Higgs scenario is a variety of scalars which could be probed at future collider experiments and a possible dark matter candidate. In this paper, we study perturbative unitarity in this model and show that, in general, the extended scalar sector of the Private Higgs model tends to soften the constraints on the Standard Model-like Higgs boson mass. We then calculate the annihilation cross sections of dark matter in this model and find that one can easily account for the observed density of dark matter in the Universe with relatively natural values of the model's parameters. Finally, we investigate the possibility of detecting Private Higgs dark matter indirectly via the observation of anomalous gamma rays originating from the galactic halo. We show that a substantial flux of photons can be produced from the annihilation of Private Higgs dark matter such that, if there is considerable clumping of dark matter in the galactic halo, the flux of these gamma rays could be observed by ground-based telescope arrays such as VERITAS and HESS.

*Electronic address: cbjackson@bnl.gov

I. INTRODUCTION

One of the most puzzling issues in the Standard Model is the large hierarchy observed in the masses of fermions. For example, in the quark sector alone, the masses of the heaviest (top) and lightest (up) quarks are separated by nearly five orders of magnitude. Conversely, if one assumes that all fermions receive their mass via interactions with the *same* Higgs doublet (as in the Standard Model (SM)), the large hierarchy of masses observed in the fermion sector translates into a large hierarchy in the Yukawa couplings of the fermions.

Recently, it has been proposed that the hierarchy of fermion masses can be made natural by extending the scalar sector of the SM to include one Higgs doublet (or *Private Higgs* (PH)) per fermion [1]. In this scenario, all of the Yukawa couplings can be made of $\mathcal{O}(1)$ by tuning parameters of the model. In other words, the vacuum expectation values (vev's) of each respective PH field can be made to satisfy $v_f \sim m_f$ such that the hierarchy in the fermion mass spectrum becomes natural.

The approach to electroweak symmetry breaking (EWSB) in the PH model is quite different than those of other multi-Higgs models. First, one introduces a gauge singlet scalar S and uses its vev along with certain interactions between this field and the various PH fields to induce “negative-mass-squared” instabilities. By using different terms in the Lagrangian for the top PH and non-top PH fields, one can easily explain the hierarchy in vev's by tuning certain parameters of the model. As a consequence of this approach, the lighter the fermion is, the heavier its associated PH particle must be in order to explain the smallness of the respective vev. In particular, the mass of the PH particle associated with the up quark can be shown to lie in the $10^2 - 10^3$ TeV range which is definitely beyond the reach of the Large Hadron Collider (LHC). However, there is interesting phenomenology originating from the sector of the top and bottom PH fields along with the singlet scalar. In particular, the physical spectrum of this sector will contain two light scalar Higgs boson (which are admixtures of the singlet scalar and top PH fields), a heavy scalar Higgs, a charged Higgs and a pseudoscalar. The last three arise from the bottom PH field and all have masses in the \sim TeV range. While we will focus mainly on the light scalars in this work, the heavier Higgs bosons could be probed at the LHC via production with bottom quarks (since the Yukawa coupling between the bottom quarks and the bottom PH field is

of order unity)¹.

In order to avoid introducing tree-level flavor-changing neutral currents (FCNC's), the quark sector of the PH model contains a set of six discrete symmetries for each quark flavor. Under these symmetries, the right-handed quarks, their respective PH fields and S are all odd, while all other SM fields are even. The existence of these discrete symmetries provides one of the most interesting features of the PH scenario which is the possibility of a dark matter (DM) candidate. As we will show, the features of Private Higgs dark matter (PHDM) depend on the mixing between the top PH field and the singlet scalar S . In the case where the mixing is negligible, the DM sector of the PH scenario reduces to that of previously studied singlet scalar DM scenarios [2, 3, 4, 5, 6, 7]. PHDM also shares some similarities to scalar DM which arises from the Inert Doublet Model (IDM) [8, 9, 10, 11, 12, 13, 14]. However, in the case of general mixing between the top PH and singlet fields, the features of PHDM can be quite different as we demonstrate.

After detailing the model in Section II, we first investigate the effects of the extended scalar sector of the PH model on perturbative unitarity in Section III. In the SM, applying the condition of perturbative unitarity to scattering amplitudes provides important constraints on the Higgs boson mass or the center-of-mass energy at which the theory breaks down (for large Higgs boson masses). As we show, the constraints on the SM-like Higgs mass can be softened significantly in the PH scenario depending on the masses and mixings between the top PH and S .

Next, in Section IV, we consider dark matter in the PH model for general mixing between the singlet scalar and the top PH field. Utilizing the observations from WMAP [15], we show that the PH model is able to account for all of the observed dark matter in the Universe for relatively natural values of the model's parameters. In addition, in Section IV A, we consider the possibility of detecting PHDM via its annihilation into anomalous gamma rays in the galactic halo. We show that, with a favorable distribution of DM in the halo, PHDM could be detected by ground-based telescopes, but is probably beyond the reach of the space-based GLAST telescope [16]. Finally, in Section V, we conclude.

¹ Presumably, the PH partner of the τ could also provide interesting phenomenology; however, we will focus on the quark sector here.

II. THE MODEL

The main goal of the Private Higgs model is to account for the extremely large hierarchy observed in the fermion mass spectrum [1]. For purposes of this paper, we will focus on the quark sector. In contrast to the SM, where one introduces a single scalar doublet which couples to all quarks, the PH scenario democratically introduces one Higgs doublet ϕ_q ($q = u, d, s, c, t, b$) per quark. All of the PH fields are assumed to have identical $SU(2) \times U(1)$ quantum numbers as the SM Higgs. In order to avoid tree-level FCNC's, a set of six separate discrete symmetries K_q are introduced to eliminate *cross talk* between quarks of different flavors [17]. In addition to the PH fields, one also introduces a gauge singlet scalar field S which also transforms under K_q . Specifically, the right-handed quarks (U_R, D_R) along with the PH fields and S are all odd under K_q , i.e.:

$$U_R \rightarrow -U_R \ (D_R \rightarrow -D_R) \ , \ \phi_q \rightarrow -\phi_q \ , \ S \rightarrow -S \ , \quad (1)$$

while all other fields are considered even under K_q . The Lagrangian which is symmetric under the K_q symmetries is then given by:

$$\begin{aligned} \mathcal{L} = & \mathcal{L}_{SM-H} - \sum_q (y_D^{PH} \bar{Q}_L \phi_D D_R + y_U^{PH} \bar{Q}_L \tilde{\phi}_U U_R) \\ & + \partial_\mu S \partial^\mu S + \sum_q [(D_\mu \phi_q)^\dagger D^\mu \phi_q - V(S, \phi_q)] \ , \end{aligned} \quad (2)$$

where $\tilde{\phi}_U = i\sigma_2 \phi_U$ and \mathcal{L}_{SM-H} is the SM Lagrangian without the Higgs terms. The scalar potential $V(S, \phi_q)$ is given by:

$$\begin{aligned} V(S, \phi_q) = & \frac{\lambda_S}{4} \left(S^2 - \frac{v_d^2}{2} \right)^2 + \sum_q \left(\frac{1}{2} M_{\phi_q}^2 \phi_q^\dagger \phi_q + \lambda_q (\phi_q^\dagger \phi_q)^2 - g_{sq} S^2 \phi_q^\dagger \phi_q \right) \\ & - \sum_{q \neq q'} \left(\frac{\gamma_{qq'}}{\sqrt{2}} v_s S \phi_q^\dagger \phi_{q'} + a_{qq'} \phi_q^\dagger \phi_{q'} \phi_q^\dagger \phi_{q'} + b_{qq'} \phi_q^\dagger \phi_q \phi_{q'}^\dagger \phi_{q'} + c_{qq'} \phi_q^\dagger \phi_{q'} \phi_{q'}^\dagger \phi_q \right) + h.c. \ , \end{aligned} \quad (3)$$

where, for stability of the potential, $a_{qq'}, b_{qq'}, c_{qq'} < 0$. In our analysis, we will assume these terms are small and neglect them in the following. Note that v_d is a free parameter and should not be confused with the vev of S given by v_s (see below).

In the PH model, instead of inducing EWSB through the usual ‘‘negative-mass-squared’’ approach where $M_{\phi_q}^2 < 0$, one utilizes the vev of the singlet field S (v_s). In particular, for the top PH one assumes $M_{\phi_t}^2 > 0$ and induces EWSB through the g_{st} coupling and

v_s . Thus, taking $g_{st} > 0$ and $\frac{1}{2}M_{\phi_t}^2 - g_{st}v_s^2 \equiv \mu_t^2 < 0$, the top PH is forced to develop a negative-mass-squared instability which, in turn, spontaneously breaks the $SU(2)_L \times U(1)_Y$ symmetry. Therefore, in a sense, the top PH plays the role of the SM Higgs.

In general, the PH scenario can contain many new free parameters in addition to those of the SM. In order to simplify our analysis in the following sections, we will make a succession of approximations. Thus, our results will not probe the full parameter space of the PH scenario, but should be viewed as a first step in this direction. To begin, we will assume that $M_{\phi_t}^2 \ll g_{st}v_s^2$ which is in accordance with the symmetry breaking pattern discussed above. Then, the potential in the $S - \phi_t$ sector becomes:

$$V(S, \phi_t) = \frac{\lambda_S}{4} \left(S^2 - \frac{v_d^2}{2} \right)^2 + \lambda_t (\phi_t^\dagger \phi_t)^2 - g_{st} S^2 \phi_t^\dagger \phi_t. \quad (4)$$

Minimizing this potential, we find the conditions:

$$\left. \frac{\partial V(S, \phi_t)}{\partial S} \right|_{\langle S \rangle, \langle \phi_t \rangle} = \lambda_S \left(\langle S \rangle^2 - \frac{v_d^2}{2} \right) - 2g_{st} \langle \phi_t \rangle^2 = 0, \quad (5)$$

and:

$$\left. \frac{\partial V(S, \phi_t)}{\partial \phi_t} \right|_{\langle S \rangle, \langle \phi_t \rangle} = 2\lambda_t \langle \phi_t \rangle^2 - g_{st} \langle S \rangle^2 = 0. \quad (6)$$

Solving these equations for the individual vev's we find:

$$\langle S \rangle^2 = \frac{v_d^2}{2} \left(\frac{\lambda_S \lambda_t}{\lambda_S \lambda_t - g_{st}^2} \right) \equiv \frac{v_S^2}{2}, \quad (7)$$

for the vev of S and for the top PH vev:

$$\langle \phi_t \rangle^2 = \frac{v_d^2}{4} \left(\frac{g_{st} \lambda_S}{\lambda_S \lambda_t - g_{st}^2} \right) \equiv \frac{v_h^2}{2}. \quad (8)$$

We also note the relationship between v_s and v_h :

$$v_h^2 = \frac{g_{st}}{2\lambda_t} v_s^2. \quad (9)$$

Next, we consider the non-top PH fields which acquire their vev's in a slightly different manner. First, as in the case of the top PH, the mass parameter $M_{\phi_q}^2$ is assumed to be positive. However, for the ϕ_q fields (where $q \neq t$), one imposes the condition $M_{\phi_q}^2 > g_{sq}v_s^2$ in contrast to the case of the top PH. Then, vev's for the non-top PH fields are induced through the cubic term $\gamma_{qq'}$ and the vev's v_s and v_h . Again, to simplify our analysis, we will make some assumptions. Specifically, we will assume that:

$$M_{\phi_q}^2 \gg g_{st}v_s^2, \quad \lambda_q \quad (10)$$

which is consistent with the symmetry breaking pattern discussed above. Then, after S and ϕ_t pick up vev's, the relevant part of the ϕ_q potential is:

$$\frac{1}{2}M_{\phi_q}^2\phi_q^\dagger\phi_q - \frac{\gamma_{qt}}{\sqrt{2}}\frac{v_h v_s^2}{2}\phi_q. \quad (11)$$

Minimizing this potential, the vev's for the non-top Higgs fields are:

$$\langle\phi_q\rangle = \frac{\gamma_{qt}}{\sqrt{2}}\frac{v_h v_s^2}{M_{\phi_q}^2} \equiv v_q. \quad (12)$$

Eq. (12) summarizes the main result of the PH scenario. By having the parameter γ_{qt} to be small while keeping $M_{\phi_q}^2$ large, one is able to make *all* Yukawa couplings (which are given by m_q/v_q) of $\mathcal{O}(1)$ without fine-tuning. As a consequence of this relation, from Eq. (12), one can show that the lighter quarks have associated PH particles in the $10^2 - 10^3$ TeV range which are definitely beyond the reach of current or future experiments. However, the masses from the $\phi_t - S$ sector can be naturally light (100's GeV), while the bottom PH particle can have masses in the TeV range. In the next section, we will study the S, ϕ_t, ϕ_b sector in detail.

Finally, inserting Eqs. (8) and (12) into the Lagrangian of Eq. (2), it is easy to show that the W^\pm mass is given in the PH model by:

$$m_W^2 = \frac{1}{2}g v_h^2 \left[1 + \sum_{q \neq t} \left(\frac{v_q^2}{v_h^2} \right) \right]. \quad (13)$$

Obviously, the leading term in the sum comes from the bottom PH; however, even in this case, the contribution is of order $m_b^2/m_t^2 \sim 0.001$. Thus, the contributions to EWSB from quarks lighter than the top are negligible and our statement above that the role of the SM Higgs boson is being played by the top PH is verified.

A. Mass Eigenstates and Their Interactions

Under the assumptions we have made above, the scalar potential in the S, ϕ_t, ϕ_b sector reduces to:

$$\begin{aligned} V(S, \phi_t, \phi_b) = & \frac{\lambda_S}{4} \left(S^2 - \frac{v_d^2}{2} \right)^2 + \lambda_t (\phi_t^\dagger \phi_t)^2 - g_{st} S^2 \phi_t^\dagger \phi_t \\ & + \frac{1}{2} M_{\phi_b}^2 \phi_b^\dagger \phi_b - \frac{\gamma_{tb}}{\sqrt{2}} v_s S (\phi_t^\dagger \phi_b + \phi_b^\dagger \phi_t). \end{aligned} \quad (14)$$

To begin, we expand the PH Higgs fields in the usual way:

$$\phi_t = \begin{pmatrix} \omega^+ \\ \frac{1}{\sqrt{2}}(v_h + h_t + i\chi^0) \end{pmatrix}, \quad (15)$$

$$\phi_b = \begin{pmatrix} H^+ \\ v_b + H_b + iA_b \end{pmatrix}, \quad (16)$$

while the singlet field is expanded as:

$$S = \frac{1}{\sqrt{2}}(v_s + \sigma). \quad (17)$$

In the above expansions, ω^\pm and χ^0 are assumed to play the roles of the usual Goldstone bosons which are eaten by the W^\pm and Z , while H^\pm and A_b are charged and pseudoscalar Higgs bosons, respectively. Both the H^\pm and A_b will have masses on the order of $M_{\phi_b} \sim \text{TeV}$ and could provide interesting phenomenology at the LHC. Note that we are neglecting mixing between the ‘‘pure Goldstones’’ (ω^\pm, χ^0) and the ‘‘physical Higgs bosons’’ (H^\pm, A_b). These mixings are typically of order $\frac{\gamma_{tb}v_b^2}{M_{\phi_b}^2}$ and, thus, are extremely small.

Inserting the expansions of the Higgs fields from Eqs. (15) - (17) into (14), we first extract the mass terms of the Goldstone bosons which we require to vanish:

$$m_{\omega^\pm}^2 = m_{\chi^0}^2 = \lambda_t v_h^2 - \frac{1}{2} g_{st} v_s^2 = 0. \quad (18)$$

Note that this equation is in agreement with Eq. (9).

Next, we extract the mass-squared matrix in the (h_t, σ, H_b) basis defined through:

$$V \sim \frac{1}{2} \begin{pmatrix} h_t & \sigma & H_b \end{pmatrix} \mathcal{M}_0^2 \begin{pmatrix} h_t \\ \sigma \\ H_b \end{pmatrix}, \quad (19)$$

where:

$$\mathcal{M}_0^2 = \begin{pmatrix} 2\lambda_t v_h^2 & -\frac{1}{2} g_{st} v_h v_s & -\frac{\gamma_{tb} v_s^2}{2\sqrt{2}} \\ -\frac{1}{2} g_{st} v_h v_s & \frac{1}{2} \lambda_S v_s^2 & -\frac{\gamma_{tb} v_h v_s}{2\sqrt{2}} \\ -\frac{\gamma_{tb} v_s^2}{2\sqrt{2}} & -\frac{\gamma_{tb} v_h v_s}{2\sqrt{2}} & M_{\phi_b}^2 \end{pmatrix}. \quad (20)$$

Instead of diagonalizing the full 3×3 matrix, we choose to utilize the above assumptions and diagonalize perturbatively. First, consider the mixing between h_t and H_b where the

mixing angle in this sector can be given by:

$$s_{tb} \equiv \sin \theta_{tb} \simeq \frac{\gamma_{tb} v_s^2}{\sqrt{2} M_{\phi_b}^2} \equiv \frac{v_b}{v_h}, \quad (21)$$

while $c_{tb} \equiv \cos \theta_{tb} \simeq 1$. Similarly, the mixing between σ and H_b is described by the angle:

$$s_{\sigma b} \equiv \sin \theta_{\sigma b} \simeq \frac{\gamma_{tb} v_h v_s}{\sqrt{2} M_{\phi_b}^2} \equiv \frac{v_b}{v_s} \quad (22)$$

with $c_{\sigma b} \equiv \cos \theta_{\sigma b} \simeq 1$. Note that, by construction, $v_b \ll v_t, v_s$ such that the above mixing angles are indeed very small and, thus, our perturbative treatment is justified.

Next, we consider the mixing in the $h_t - \sigma$ sector. We define the mixing angle β through the unitary matrix which diagonalizes the mass matrix in this sector as:

$$U = \begin{pmatrix} c_\beta & s_\beta \\ -s_\beta & c_\beta \end{pmatrix}, \quad (23)$$

where $c_\beta(s_\beta) \equiv \cos \beta(\sin \beta)$. Using this matrix to diagonalize the mass matrix in the $h_t - \sigma$ sector, we find the mass eigenvalues are:

$$m_{h^0}^2 = 2\lambda_t c_\beta^2 v_h^2 + \frac{\lambda_S}{2} s_\beta^2 v_s^2 - \frac{g_{st}}{2} s_\beta c_\beta v_h v_s, \quad (24)$$

and:

$$m_{K^0}^2 = 2\lambda_t s_\beta^2 v_h^2 + \frac{\lambda_S}{2} c_\beta^2 v_s^2 + \frac{g_{st}}{2} s_\beta c_\beta v_h v_s. \quad (25)$$

Finally, requiring the off-diagonal elements of the diagonalized matrix to vanish, we have:

$$0 = -\frac{(c_\beta^2 - s_\beta^2)}{2} (g_{st} v_h v_s) - s_\beta c_\beta \left(2\lambda_t v_h^2 - \frac{\lambda_S}{2} v_s^2 \right). \quad (26)$$

In this work, we find it convenient to exchange some of the original parameters of the PH model for those of the physical masses and mixing parameters. In particular, solving Eqs. (24)-(26) for λ_S and λ_t in terms of the masses m_{h^0} and m_{K^0} as well as the mixing angle β , we find:

$$\lambda_S = \frac{1}{v_s^2} \left[(m_{h^0}^2 + m_{K^0}^2) - (m_{h^0}^2 - m_{K^0}^2) \cos 2\beta \right], \quad (27)$$

$$\lambda_t = \frac{1}{4v_h^2} \left[(m_{h^0}^2 + m_{K^0}^2) + (m_{h^0}^2 - m_{K^0}^2) \cos 2\beta \right], \quad (28)$$

while we use Eq. (9) to determine g_{st} :

$$g_{st} = 2\lambda_t \left(\frac{v_h}{v_s} \right)^2. \quad (29)$$

Thus, in the following, we will describe the PH scalar sector in terms of the SM Higgs vev (v_h), the vev of S (v_s), the physical scalar masses ($m_{h^0}, m_{K^0}, M_{\phi_b}$) and the mixing parameters (β, γ_{tb}). Note that v_h is set by the mass of the SM W^\pm (see Eq. (13)), while the parameters associated with the bottom PH (M_{ϕ_b}, γ_{tb}) will play only a minor role in our analysis.

Using the mixing angles defined above, we can expand the original fields (h_t, σ, H_b) in terms of the mass eigenstates (h^0, K^0, H^0) as (to linear order in the small mixing angles):

$$h_t = c_\beta h^0 + s_\beta K^0 + s_{tb} H^0, \quad (30)$$

$$\sigma = c_\beta K^0 - s_\beta h^0 + s_{\sigma b} H^0, \quad (31)$$

$$H_b = (1 - s_{\sigma b} c_\beta) H^0 + (s_{\sigma b} s_\beta - s_{tb} c_\beta) h^0 - s_{tb} s_\beta K^0. \quad (32)$$

The three-point and four-point couplings between the various mass eigenstates are given in the appendix. Note that, for small values of β , the mass eigenstate K^0 will be mostly made of the singlet scalar σ and, thus, could provide a possible dark matter candidate (see Section IV).

Finally, one might expect that relatively small values of m_{K^0} would have been excluded by the LEP II data. In general, the mostly singlet K^0 could have been produced at LEP through the SM-like process $e^+e^- \rightarrow ZK^0$. However, for the small values of β which we consider, the cross section for production of K^0 in association with a SM Z in e^+e^- collisions scales as:

$$\sigma(e^+e^- \rightarrow ZK^0) \simeq s_\beta^2 \sigma(e^+e^- \rightarrow Zh_{SM}). \quad (33)$$

where h_{SM} is the SM Higgs boson. Therefore, in the small β regime, the production cross section is strongly suppressed and should be well below the experimental limits from the LEP II data [18].

III. PERTURBATIVE UNITARITY IN THE PH MODEL

In the SM, imposing perturbative unitarity on scattering amplitudes provides important constraints on the mass of the Higgs boson and the center-of-mass energy at which the theory breaks down [19]. In this section, we apply the condition of perturbative unitarity to the PH model and study the effects in relation to those of the SM.

The approach to studying perturbative unitarity in scattering amplitudes is traditionally performed in terms of partial waves where one expands the amplitude for a given process as:

$$\mathcal{A} = 16\pi \sum_{\ell=0}^{\infty} (2\ell + 1) P_{\ell}(\cos \theta) a_{\ell}, \quad (34)$$

where a_{ℓ} is the spin ℓ partial wave and $P_{\ell}(\cos \theta)$ are the Legendre polynomials. Squaring the amplitude and using the orthogonality of the Legendre polynomials, the cross section can be written as:

$$\sigma = \frac{16\pi}{s} \sum_{\ell=0}^{\infty} (2\ell + 1) |a_{\ell}|^2. \quad (35)$$

Then, using the optical theorem, the condition of perturbative unitarity can be imposed by writing:

$$\sigma = \frac{16\pi}{s} \sum_{\ell=0}^{\infty} (2\ell + 1) |a_{\ell}|^2 = \frac{1}{s} \text{Im}[\mathcal{A}(\theta = 0)]. \quad (36)$$

where $\mathcal{A}(\theta = 0)$ indicates the scattering amplitude in the forward direction. Using Eq. (34), this implies:

$$|\text{Re}(a_{\ell})| \leq \frac{1}{2}. \quad (37)$$

In the SM, imposing perturbative unitarity on $h_{SM}h_{SM} \rightarrow h_{SM}h_{SM}$ scattering gives a direct probe of the Higgs self couplings [19]. Let us consider the effects of the extended scalar sector of the PH scenario on the related channel $h^0h^0 \rightarrow h^0h^0$. In particular, we focus on the $J = 0$ partial wave amplitude a_0 for this process which is given by:

$$a_0 = \frac{1}{16\pi s\beta^2} \int_{-s\beta^2}^0 \mathcal{A}(h^0h^0 \rightarrow h^0h^0) dt, \quad (38)$$

² We also considered other channels including scattering amplitudes between longitudinal gauge bosons as well as those between the different PH particles. In the end, we found similar effects as those presented here for $h^0h^0 \rightarrow h^0h^0$ scattering.

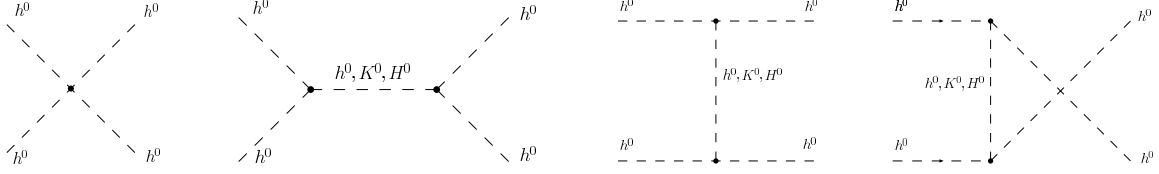


FIG. 1: Feynman diagrams for $h^0 h^0 \rightarrow h^0 h^0$ scattering.

where \sqrt{s} is the center-of-mass energy and $\beta^2 = 1 - \frac{4m_{h^0}^2}{s}$. The Feynman diagrams which contribute to $h^0 h^0$ scattering in the PH model are shown in Fig. 1. In terms of the couplings given in the appendix, the $J = 0$ partial wave amplitude is:

$$\begin{aligned}
 a_0 = & -\frac{1}{32\pi} \left\{ g_{h^0 h^0 h^0 h^0} + \frac{g_{h^0 h^0 h^0}^2}{s - m_{h^0}^2} + \frac{g_{h^0 h^0 K^0}^2}{s - m_{K^0}^2} + \frac{g_{h^0 h^0 H^0}^2}{s - m_{H^0}^2} - \frac{2}{s\beta^2} \left[g_{h^0 h^0 h^0}^2 \ln\left(\frac{s}{m_{h^0}^2} - 3\right) \right. \right. \\
 & \left. \left. + g_{h^0 h^0 K^0}^2 \ln\left(\frac{s - 4m_{h^0}^2 + m_{K^0}^2}{m_{K^0}^2}\right) + g_{h^0 h^0 H^0}^2 \ln\left(\frac{s - 4m_{h^0}^2 + m_{H^0}^2}{m_{H^0}^2}\right) \right] \right\}. \quad (39)
 \end{aligned}$$

Note that, using the expressions for the couplings in the appendix along with Eqs. (27)-(29), one can show that this expression reduces to the correct SM result when $\beta = 0$ [19].

Now, we take the limit where $s \gg m_{h^0}^2, m_{K^0}^2, m_{H^0}^2$. In the SM, this limit allows one to extract the mass of the Higgs boson where perturbative unitarity is violated. The $J = 0$ partial wave amplitude in this limit reduces to the four-point interaction:

$$\lim_{s \rightarrow \infty} a_0 = -\frac{1}{32\pi} g_{h^0 h^0 h^0 h^0}. \quad (40)$$

In the SM limit (where $\beta \rightarrow 0$), we can use this expression to constrain the mass of the Higgs boson [19]³:

$$|a_0| \leq \frac{1}{2} \rightarrow m_{h^0} \leq \sqrt{\frac{16\pi}{3}} v_h \simeq 1007 \text{ GeV}. \quad (41)$$

In Fig. 2, we plot Eq. (40) as a function of the SM-like Higgs mass (m_{h^0}) for several different values of the mixing parameter β . For reference, we also plot the SM limit ($\beta = 0$). We see that, in general, the affect of the PH scalar sector is to relax the bound on the SM-like Higgs boson mass especially for larger mixing angles where the bound approaches

³ Note that tighter constraints can be provided by other channels such as $W_L W_L \rightarrow W_L W_L$. We have chosen this particular channel just as an illustration of the effects from the extended scalar sector of the PH model.

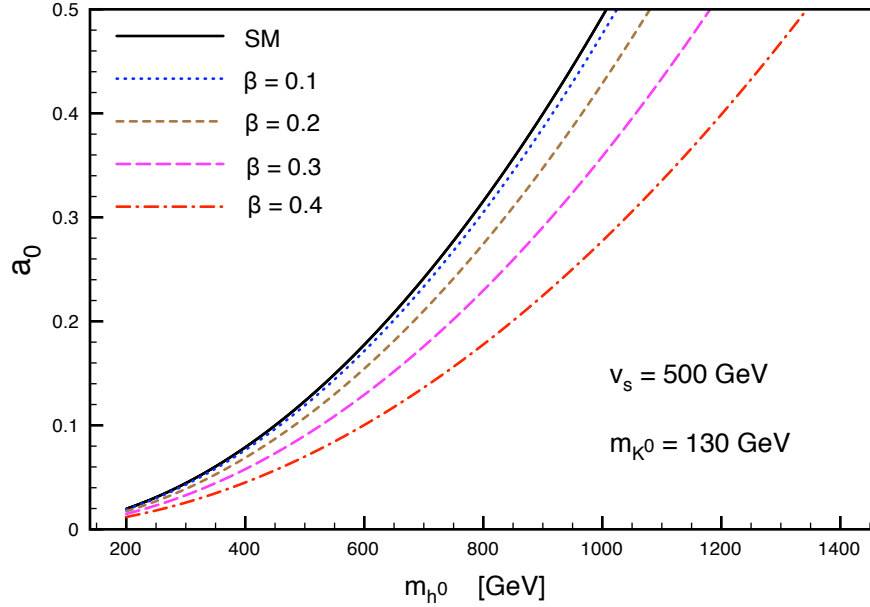


FIG. 2: The $J = 0$ partial wave amplitude for $h^0 h^0 \rightarrow h^0 h^0$ as a function of the light scalar mass m_{h^0} and the mixing parameter β .

the ~ 1.5 TeV level. We have studied the effects as a function of the K^0 mass and found that they are nearly independent of the value m_{K^0} for the ranges we consider in this paper.

IV. PRIVATE HIGGS DARK MATTER

As mentioned earlier, one of the most interesting aspects of the PH scenario is the prospect of a Weakly Interacting Massive Particle (WIMP) with masses in the expected natural range for DM. In this context, the PH model is similar to other scalar DM models such as the gauge singlet models of Refs. [2, 3, 4, 5, 6, 7] and the Inert Doublet Model (IDM) [8, 9, 10, 11, 12, 13, 14]. In this section, we calculate the annihilation cross sections of PHDM into SM particles and show that, for relatively natural values of the model parameters, one can account for all of the observed dark matter in the Universe. We also investigate the possibility of indirectly detecting PHDM via its annihilation into *anomalous* gamma rays in the galactic halo.

First, let us consider the present relic abundance of PHDM in the Universe. In the following, we will assume small values of the mixing parameter β such that K^0 is stable

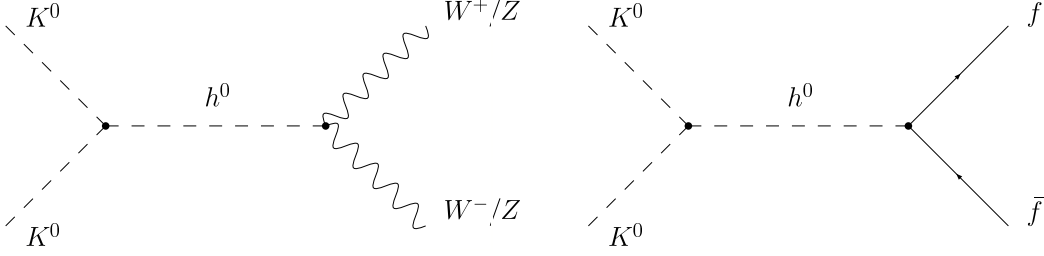


FIG. 3: Leading s -channel processes which maintain the singlet scalar K^0 in equilibrium with the rest of the cosmic fluid.

against decay into SM particles. In the early Universe, the mostly singlet Higgs boson K^0 would have been in equilibrium with the rest of the cosmic fluid. This equilibrium is maintained via K^0 pair-annihilation and pair-creation reactions. The leading $2 \rightarrow 2$ s -channel reactions which contribute to these processes are shown in Fig. 3⁴.

The present relic abundance of PHDM is determined by the pair-annihilation rates in the non-relativistic limit. The rates for each allowed channel are given in the non-relativistic limit as:

$$a(X) \equiv \lim_{u \rightarrow 0} \sigma(K^0 K^0 \rightarrow X) u \quad (42)$$

where u is the relative velocity of the annihilating particles. The total annihilation cross section is then given by summing over each of the allowed channels. Computing the cross sections for the diagrams in Fig. 4, we find:

$$a(W^+W^-) = \frac{g_{K^0 K^0 h^0}^2}{2\pi v_h^2} \frac{\sqrt{1 - \mu_w}}{(4m_{K^0}^2 - m_{h^0}^2)^2 + \Gamma_h^2 m_{h^0}^2} \left(1 - \mu_w + \frac{3}{4}\mu_w^2\right), \quad (43)$$

$$a(ZZ) = \frac{g_{K^0 K^0 h^0}^2}{4\pi v_h^2} \frac{\sqrt{1 - \mu_z}}{(4m_{K^0}^2 - m_{h^0}^2)^2 + \Gamma_h^2 m_{h^0}^2} \left(1 - \mu_z + \frac{3}{4}\mu_z^2\right), \quad (44)$$

$$a(f\bar{f}) = \frac{g_{K^0 K^0 h^0}^2}{4\pi v_h^2} \frac{(1 - \mu_f)^{\frac{3}{2}}}{(4m_{K^0}^2 - m_{h^0}^2)^2 + \Gamma_h^2 m_{h^0}^2}, \quad (45)$$

where the expression for the coupling $g_{K^0 K^0 h^0}$ can be found in the appendix, $\mu_i = m_i^2/m_{K^0}^2$ and Γ_h is the width of the h^0 for which we use SM values.

⁴ Note that we have neglected diagrams which involve the couplings of K^0 to ordinary SM matter. The contribution from these diagrams are of order s_β^2 and are thus negligible for values of β we consider.

The WMAP collaboration [15] provides a very precise determination of the present DM abundance which, at the two-sigma level, is given by:

$$\Omega_{DM}h^2 = 0.111 \pm 0.018. \quad (46)$$

As shown in Ref. [20], for a generic model of DM, the present abundance of DM is mainly determined by J_0 (the angular momentum of the dominant partial wave contributing to DM annihilation) and the annihilation cross section. In contrast, the relic abundance depends only weakly on the mass or spin of the DM particle. Thus, the very precise constraints from WMAP on $\Omega_{DM}h^2$ translate into very precise constraints on the quantity $a \equiv \sum_X a(X)$ depending on the value of J_0 . In particular, for an “s-wave annihilator” ($J_0 = 0$) such as the case considered here, the WMAP measurement translates into the bounds:

$$a = 0.8 \pm 0.1 \text{ pb}, \quad (47)$$

nearly independent of the mass or spin of the DM particle (see Fig. 1 of Ref. [20]).

In Fig. 4, we plot the values of $a(X)$ for two different scenarios: one in which the K^0 is light and only annihilates mainly into bottom quarks and tau leptons and one in which the K^0 is heavy enough to annihilate into W^+W^- and ZZ pairs. The horizontal dashed lines in the plots indicate the limits on $a(X)$ from Eq. (47). We see from the top plot that, in the light K^0 scenario and for our choice of parameters, the mass of the K^0 needed to account for the present DM abundance must lie in the narrow range of 50 to 75 GeV range depending on the value of β . In contrast, the mass of K^0 is much less constrained in the heavy K^0 scenario as can be seen from the bottom plot of Fig. 4. Note that, in this scenario, the mixing angle must be taken to be quite smaller in order to account for the present DM abundance. Finally, it should be noted that in both cases, these plots are only meant to show that for relatively natural values of the model parameters it is indeed possible to account for the observed density of DM in the Universe. A full scan of the PH parameter space would probably find other choices of parameters which could fulfill the constraints from Eq. (47).

A. Indirect Detection of PHDM

Next, we would like to investigate the possibility of detecting PHDM. We will focus here on indirect detection and save an analysis of direct detection for future work.

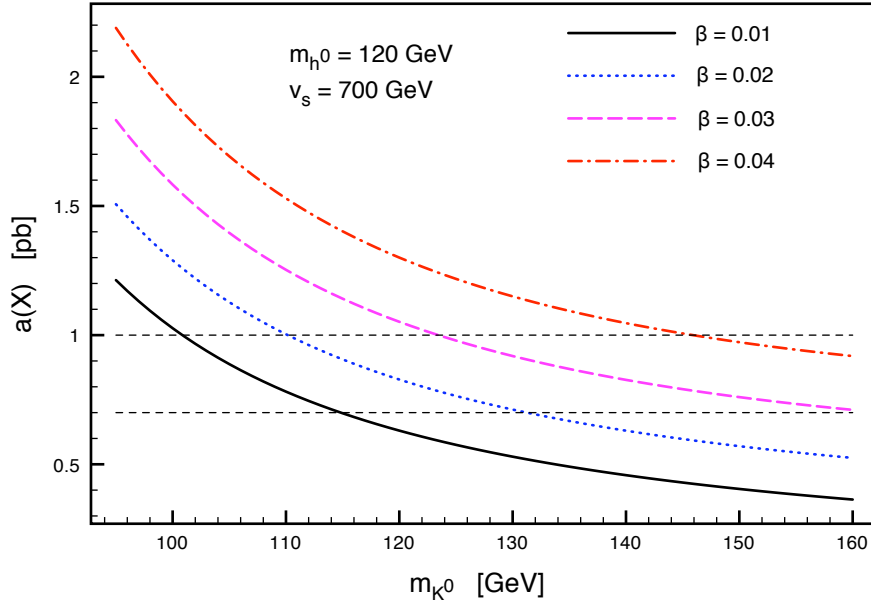
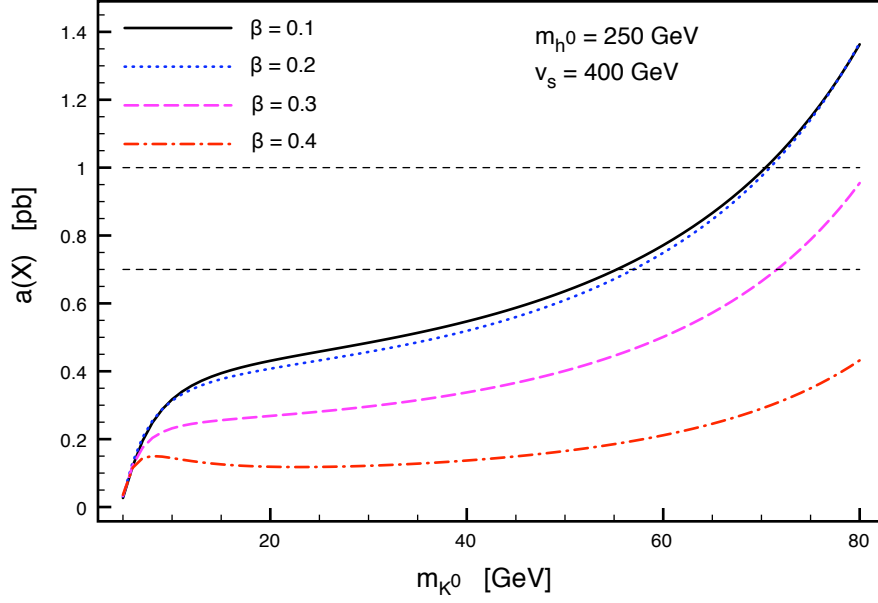


FIG. 4: The annihilation cross section as a function of the K^0 mass and the mixing parameter β . The dashed horizontal lines indicate the WMAP constraints on the annihilation cross sections given by Eq. 47.

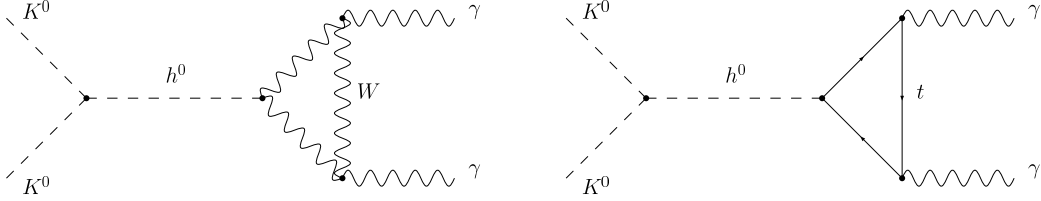


FIG. 5: Diagrams which dominate photon pair-production in the K^0 annihilation in the galactic halo.

As we have seen, the annihilation rates for PHDM are approximately velocity-independent in the non-relativistic regime. In general, this implies that DM collected in galactic halos has a substantial probability to pair-annihilate resulting in anomalous high-energy cosmic rays which can be distinguished from astrophysical backgrounds. In particular, gamma rays from these annihilations provide a chance to extract information about DM, since they can travel over galactic scales without scattering.

The production of gamma rays from $K^0 K^0$ annihilation can originate from several different processes (including hadronization, factorization and radiation from final-state particles). However, for simplicity, we will assume the dominate source is from direct annihilation into a two-body final state as shown in Fig. 5⁵. Note that, under our assumptions, only SM particles circulate the loop. In the full parameter space of the PH model, it would be possible to have charged Higgs circulating the loop. However, their couplings to h^0 are *always* of order v_b/v_h or v_b/v_s and, thus, can be safely ignored in comparison to the SM loops. The cross section for photon pair-production in the PH scenario can be written as:

$$\sigma_{\gamma\gamma} u = \frac{2g_{K^0 K^0 h^0}^2}{(s - m_{h^0}^2)^2 + \Gamma_h m_{h^0}^2} \frac{\hat{\Gamma}(h \rightarrow \gamma\gamma)}{\sqrt{s}}, \quad (48)$$

where the expression for $g_{K^0 K^0 h^0}$ is given in the appendix and, in the non-relativistic regime, $s \simeq 4m_{K^0}^2$. The hat on $\hat{\Gamma}$ indicates that one should replace $m_{h^0} \rightarrow \sqrt{s}$ in the standard expressions for on-shell Higgs decays. The expressions needed to construct $\hat{\Gamma}(h \rightarrow \gamma\gamma)$ can be found in several reviews (e.g., see Ref. [21]) and, hence, we will not repeat them here.

Next, we would like to compute the flux of photons observed on Earth from K^0 annihilation in the galactic halo. The monochromatic flux due to the $\gamma\gamma$ final state, observed by

⁵ Here, we concentrate on the dominant $\gamma\gamma$ signal and save a discussion of the $Z\gamma$ and/or $h^0\gamma$ channels for future work.

a telescope with a line of sight parameterized by $\Psi = (\theta, \phi)$ and a field of view $\Delta\Omega$ can be written as [22]:

$$\Phi = (1.1 \times 10^{-9} \text{ s}^{-1} \text{ cm}^{-2}) \left(\frac{\sigma_{\gamma\gamma u}}{1 \text{ pb}} \right) \left(\frac{100 \text{ GeV}}{m_{K^0}} \right) \bar{J}(\Psi, \Delta\Omega) \Delta\Omega, \quad (49)$$

where the dependence of the flux on the halo dark matter density distribution is contained in \bar{J} . Many models predict a large spike in the DM density in the neighborhood of the galactic center, making the line of sight towards the center of the galaxy the preferred one. However, the features of the peak are highly model-dependent resulting in values of \bar{J} ranging from 10^3 to 10^7 for $\Delta\Omega = 10^{-3}$ sr (typical for ground-based atmospheric Cherenkov telescopes) [23, 24, 25, 26].

The monochromatic photon flux predicted from PHDM annihilation in both the “light K^0 ” and “heavy K^0 ” scenarios is shown in Fig. 6. For these plots, we have assumed there is no substantial spiking in the galactic center (i.e., $\bar{J}\Delta\Omega = 1$). In the energy range corresponding to the “light K^0 ” scenario, ground-based atmospheric Cherenkov telescopes (such as VERITAS [27] and HESS [28]) typically have a flux sensitivity down to the $10^{-11} \text{ s}^{-1} \text{ cm}^{-2}$ level. In the energy range corresponding to the “heavy K^0 ” scenario, the reach goes down to the level of $10^{-12} \text{ s}^{-1} \text{ cm}^{-2}$. On the other hand, the upcoming space-based telescope GLAST [16] is limited by statistics to the $10^{-10} \text{ s}^{-1} \text{ cm}^{-2}$ level over both energy ranges. From these plots, it is clear that without a substantial spike in the galactic center, PHDM will be difficult to observe in either ground- or space-based observatories. However, if the halo does exhibit a substantial spike or strong clumping (e.g., if $\bar{J} \geq 10^5$ at $\Delta\Omega \simeq 10^{-3}$), PHDM could be observed at ground-based telescopes in either the “light” or “heavy” scenarios.

V. CONCLUSIONS

The Private Higgs model attempts to address the large hierarchy observed in the fermion mass spectrum by introducing one Higgs doublet for each fermion. EWSB is achieved not by the usual “negative-mass-squared” approach, but by introducing a gauge singlet scalar and using the vev of this field and its interactions with the PH fields to induce instabilities. In order to avoid tree-level FCNC’s, one must also introduce a set of discrete symmetries which prevents cross-talk between the various fermions. This provides one of the most interesting features of the Private Higgs model: a possible dark matter candidate.

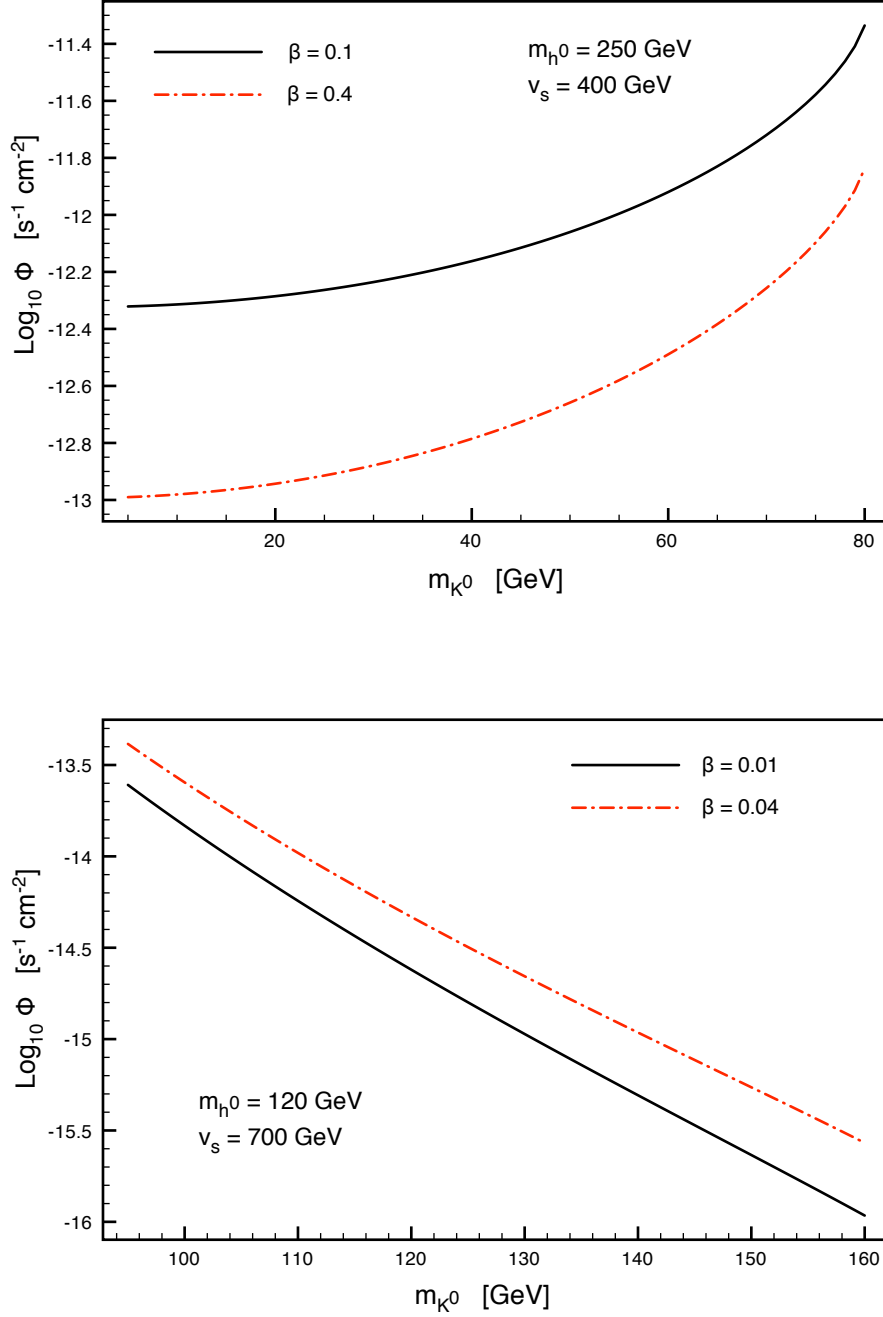


FIG. 6: The flux of monochromatic photons from the reaction $K^0 K^0 \rightarrow \gamma\gamma$ for $\bar{J}\Delta\Omega = 1$.

In this paper, we have focussed on the quark sector of the PH model with particular attention paid to the top PH, bottom PH and singlet scalar sectors. We first considered perturbative unitarity in the PH model. In the SM, one can use the requirement of unitarity of the S -matrix in scattering processes to place strong limits on the mass of the Higgs boson

or the scattering energy at which the theory breaks down. In particular, we considered the channel $h^0 h^0 \rightarrow h^0 h^0$ where we found that the general effects of the extended scalar sector of the PH model was to soften the upper bound on the SM-like Higgs boson mass.

We next considered dark matter in the PH model. For small values of the mixing between the top PH and singlet scalar, the PH model provides a candidate which can account for the relic density of dark matter observed in the present Universe. To show this, we calculated the annihilation cross section for PHDM into SM particles and compared to limits on the cross section which can be obtained from the WMAP observations. In particular, we studied two separate scenarios: one in which the PHDM particle has a mass below m_W where annihilation into bottom quarks and tau leptons dominate and one in which the PHDM mass is above this threshold where annihilation into W^+W^- and ZZ pairs dominates. In both cases, we gave examples of points in the PH parameter space where PHDM can account for the current density of dark matter.

Finally, we investigated the possibility of detecting PHDM via anomalous gamma rays originating from the annihilation of PHDM in the galactic halo. While the observation of these gamma rays may be difficult for the space-based GLAST observatory, we showed that evidence of PHDM could be observed at ground-based atmospheric Cerenkov telescopes such as VERITAS and HESS if there is substantial clustering of dark matter in the galactic halo.

Acknowledgments

The author is very grateful to Sally Dawson for a careful reading of this manuscript and many useful comments. This manuscript has been authored by employees of Brookhaven Science Associates, LLC under Contract No. DE-AC02-98CH10886 with the U.S. Department of Energy. The publisher by accepting the manuscript for publication acknowledges that the United States Government retains a non-exclusive, paid-up, irrevocable, world-wide license to publish or reproduce the published form of this manuscript, or allow others to do so, for United States Government purposes.

APPENDIX A: COUPLINGS BETWEEN MASS EIGENSTATES

Here we tabulate all of the couplings needed for our analysis. First, for $h^0 h^0 \rightarrow h^0 h^0$ scattering:

$$g_{h^0 h^0 h^0 h^0} = 4! \left(\frac{1}{4} \lambda_t c_\beta^4 + \frac{1}{16} \lambda_S s_\beta^4 - \frac{1}{4} g_{st} c_\beta^2 s_\beta^2 \right), \quad (\text{A1})$$

$$g_{h^0 h^0 h^0} = 3! \left[\lambda_t v_h c_\beta^3 - \frac{\lambda_S}{4} v_s s_\beta^3 + \frac{g_{st}}{2} c_\beta s_\beta (v_s c_\beta - v_h s_\beta) + \frac{v_s \gamma_{tb}}{\sqrt{2}} c_\beta s_\beta (s_{\sigma b} s_\beta - s_{tb} c_\beta) \right] \quad (\text{A2})$$

$$g_{h^0 h^0 K^0} = 2! \left\{ 3 \lambda_t v_h c_\beta^2 s_\beta + \frac{3}{4} \lambda_S v_s c_\beta s_\beta^2 + g_{st} \left[\frac{v_s c_\beta}{2} (3s_\beta^2 - 1) + \frac{v_h s_\beta}{2} (3c_\beta^2 - 1) \right] + \frac{v_s \gamma_{tb}}{\sqrt{2}} \left[s_{\sigma b} s_\beta (1 - 3c_\beta^2) + s_{tb} c_\beta (1 - 3s_\beta^2) \right] \right\}, \quad (\text{A3})$$

$$g_{h^0 h^0 H^0} = 2! \left[3 \lambda_t v_h s_{tb} c_\beta^2 + \frac{3}{4} \lambda_S v_s s_{\sigma b} s_\beta^2 + g_{st} \left(-\frac{1}{2} v_s s_{\sigma b} c_\beta^2 + v_s s_{tb} c_\beta s_\beta + v_h s_{\sigma b} c_\beta s_\beta - \frac{1}{2} v_h s_{tb} s_\beta^2 \right) + \frac{v_s \gamma_{tb}}{\sqrt{2}} c_\beta s_\beta \right]. \quad (\text{A4})$$

where the expressions for λ_S , λ_t and g_{st} in terms of the physical masses and SM vev (v_h) can be found in Eqs. (27)-(29).

Finally, the coupling needed in the calculation of the DM annihilation cross section is:

$$g_{K^0 K^0 h^0} = 2! \left\{ 3 \lambda_t v_h c_\beta s_\beta^2 - \frac{3}{4} \lambda_S v_s c_\beta^2 s_\beta + g_{st} \left[-\frac{v_s s_\beta}{2} (3c_\beta^2 - 1) + \frac{v_h c_\beta}{2} (3s_\beta^2 - 1) \right] + \frac{v_s \gamma_{tb}}{\sqrt{2}} \left[s_{\sigma b} c_\beta (1 - 3s_\beta^2) - s_{tb} s_\beta (1 - 3c_\beta^2) \right] \right\}. \quad (\text{A5})$$

-
- [1] R. A. Porto and A. Zee (2007), 0712.0448.
 - [2] V. Silveira and A. Zee, Phys. Lett. **B161**, 136 (1985).
 - [3] D. E. Holz and A. Zee, Phys. Lett. **B517**, 239 (2001), hep-ph/0105284.
 - [4] J. McDonald, Phys. Rev. **D50**, 3637 (1994), hep-ph/0702143.
 - [5] B. Patt and F. Wilczek (2006), hep-ph/0605188.
 - [6] O. Bertolami and R. Rosenfeld (2007), 0708.1784.
 - [7] X.-G. He, T. Li, X.-Q. Li, and H.-C. Tsai, Mod. Phys. Lett. **A22**, 2121 (2007), hep-ph/0701156.

- [8] E. Ma, Phys. Rev. **D73**, 077301 (2006), hep-ph/0601225.
- [9] R. Barbieri, L. J. Hall, and V. S. Rychkov, Phys. Rev. **D74**, 015007 (2006), hep-ph/0603188.
- [10] M. Cirelli, N. Fornengo, and A. Strumia, Nucl. Phys. **B753**, 178 (2006), hep-ph/0512090.
- [11] N. G. Deshpande and E. Ma, Phys. Rev. **D18**, 2574 (1978).
- [12] D. Majumdar and A. Ghosal (2006), hep-ph/0607067.
- [13] J. A. Casas, J. R. Espinosa, and I. Hidalgo, Nucl. Phys. **B777**, 226 (2007), hep-ph/0607279.
- [14] X. Calmet and J. F. Oliver, Europhys. Lett. **77**, 51002 (2007), hep-ph/0606209.
- [15] D. N. Spergel et al. (WMAP), Astrophys. J. Suppl. **148**, 175 (2003), astro-ph/0302209.
- [16] A. Morselli, A. Lionetto, A. Cesarini, F. Fucito, and P. Ullio (GLAST), Nucl. Phys. Proc. Suppl. **113**, 213 (2002), astro-ph/0211327.
- [17] S. L. Glashow and S. Weinberg, Phys. Rev. **D15**, 1958 (1977).
- [18] R. Barate et al. (LEP Working Group for Higgs boson searches), Phys. Lett. **B565**, 61 (2003), hep-ex/0306033.
- [19] B. W. Lee, C. Quigg, and H. B. Thacker, Phys. Rev. **D16**, 1519 (1977).
- [20] A. Birkedal, K. Matchev, and M. Perelstein, Phys. Rev. **D70**, 077701 (2004), hep-ph/0403004.
- [21] A. Djouadi, Phys. Rept. **457**, 1 (2008), hep-ph/0503172.
- [22] L. Bergstrom, P. Ullio, and J. H. Buckley, Astropart. Phys. **9**, 137 (1998), astro-ph/9712318.
- [23] J. F. Navarro, C. S. Frenk, and S. D. M. White, Astrophys. J. **490**, 493 (1997), astro-ph/9611107.
- [24] B. Moore, F. Governato, T. Quinn, J. Stadel, and G. Lake, Astrophys. J. **499**, L5 (1998), astro-ph/9709051.
- [25] B. Moore, T. Quinn, F. Governato, J. Stadel, and G. Lake, Mon. Not. Roy. Astron. Soc. **310**, 1147 (1999), astro-ph/9903164.
- [26] O. Y. Gnedin, A. V. Kravtsov, A. A. Klypin, and D. Nagai, Astrophys. J. **616**, 16 (2004), astro-ph/0406247.
- [27] T. C. Weekes et al., Astropart. Phys. **17**, 221 (2002), astro-ph/0108478.
- [28] J. A. Hinton (The HESS), New Astron. Rev. **48**, 331 (2004), astro-ph/0403052.